MOLECULAR AND CELLULAR BIOLOGY, Nov. 2009, p. 5718–5728 Vol. 29, No. 21
0270-7306/09/$12.00 doi:10.1128/MCB.00270-09
Copyright © 2009, American Society for Microbiology. All Rights Reserved.

Overlapping Functions of Nuclear Envelope Proteins NET25 (Lem2) and Emerin in Regulation of Extracellular Signal-Regulated Kinase Signaling in Myoblast Differentiation▽

Michael D. Huber, Tinglu Guan, and Larry Gerace*

Department of Cell Biology, The Scripps Research Institute, La Jolla, California 92037

Received 2 March 2009/Returned for modification 3 April 2009/Accepted 23 August 2009

Mutations in certain nuclear envelope (NE) proteins cause muscular dystrophies and other disorders, but the disease mechanisms remain unclear. The *n*uclear *e*nvelope *t*ransmembrane protein NET25 (Lem2) is a truncated paralog of MAN1, an NE component linked to bone disorders. NET25 and MAN1 share an ~40-residue LEM homology domain with emerin, the protein mutated in X-linked Emery-Dreifuss muscular dystrophy. However, roles for NET25 and MAN1 in myogenesis have not yet been described. Using RNA interference in C2C12 myoblasts, we show for the first time that both NET25 and MAN1 are required for myogenic differentiation. NET25 depletion causes hyperactivation of extracellular signal-regulated kinase 1/2 at the onset of differentiation, and pharmacological inhibition of this transient overactivation rescues myogenesis. In contrast, pharmacological inhibition of both mitogen-activated protein kinase and transforming growth factor β signaling is required to rescue differentiation after MAN1 depletion. Ectopic expression of silencing-resistant NET25 rescues myogenesis after depletion of emerin but not after MAN1 silencing. Thus, NET25 and emerin have at least partially overlapping functions during myogenic differentiation, which are distinct from those of MAN1. Our work supports the hypothesis that deregulation of cell signaling contributes to NE-linked disorders and suggests that mutations in NET25 and MAN1 may cause muscle diseases.

The nuclear envelope (NE), which forms the barrier between the nucleus and the cytoplasm, consists of the inner nuclear membrane (INM) and outer nuclear membrane, nuclear pore complexes, and the nuclear lamina. The lamina is a meshwork of intermediate type filament proteins (lamins A/C, B1, and B2) associated with numerous transmembrane proteins of the INM. The transmembrane proteins of the INM include emerin, MAN1, and NET25, the main subjects of this study. The lamina provides a scaffold for the NE and anchoring sites for chromatin and the cytoplasmic cytoskeleton and has been implicated in regulation of gene expression, DNA replication, and cell signaling (reviewed in reference 40).

Mutations in genes encoding NE proteins have been causally linked to a host of human diseases (reviewed in reference 43). The most common of these are diseases affecting mesenchyme-derived tissues, particularly cardiac and skeletal muscle. Autosomal dominant Emery-Dreifuss muscular dystrophy (EDMD) (5), limb-girdle muscular dystrophy type 1B (29), and dilated cardiomyopathy (see reference 36 and references therein) are caused by certain mutations in LMNA, the gene encoding lamins A/C. The X-linked form of EDMD results from mutations in EMD, which encodes the lamin A-binding transmembrane protein emerin (4). Although LMNA and EMD mutations account for roughly two-thirds of all reported EDMD cases, the genetic basis for the remaining third remains unknown (19).

Muscular dystrophies are diseases that result from increased muscle degeneration and/or impaired muscle regeneration. Satellite cells are the major muscle resident stem cells responsible for the regenerative capacity of postnatal muscle. Initiation of muscle regeneration involves the activation of satellite cells to form a proliferating myoblast pool (22). This is followed by the fusion of myoblasts into multinucleated myotubes and the expression of characteristic muscle proteins, like muscle creatine kinase and the skeletal muscle myosin heavy chain (MyHC) (reviewed in reference 8). Muscle-specific myogenic regulatory transcription factors (MRFs) are critical throughout muscle differentiation (8). These include Myf5 and MyoD, which are important for the early steps of myogenesis, including myoblast commitment, and MRF4 and myogenin, which control the late events of myoblast fusion and muscle-specific gene expression.

Two models have been proposed for the role of lamina mutations in disease mechanisms. One model posits that mutations in lamina proteins alter the mechanical properties of the lamina, thereby rendering the functional state of the nucleus more sensitive to physical stress. This could be particularly significant in tissues subjected to mechanical forces, such as heart and muscle. Indeed, significant changes in the mechanical properties of the nucleus have been described in cells with mutant lamina proteins (23, 25). The other model postulates that changes in the lamina alter gene expression by disrupting interactions of the lamina with chromatin regulators, such as signaling and transcription factors. This could lead to changes in the proliferation or differentiation capacity of cells, which could affect tissue regeneration or lead to cell death. Supporting this hypothesis, both lamins and INM proteins have been linked to signaling, using a variety of approaches. In the organismal context, both mechanisms could contribute to

* Corresponding author. Mailing address: Department of Cell Biology, IMM-10, The Scripps Research Institute, 10550 North Torrey Pines Road, La Jolla, CA 92037. Phone: (858) 784-8514. Fax: (858) 784-0132. E-mail: lgerace@scripps.edu.

▽ Published ahead of print on 31 August 2009.

diseases to variable degrees, depending on the protein and cell type affected (reviewed in reference 24).

A proteomics study from our laboratory identified over 50 novel potential *n*uclear *e*nvelope *t*ransmembrane proteins (NETs) (38), substantially increasing the list of ~15 integral proteins of the NE that had been identified at the time. Expression profiling suggested that some of these novel NETs might have a role in muscle differentiation and/or maintenance (9). The lamina-associated protein NET25, also known as Lem2 (6), stood out as a particularly appealing candidate for having a myogenic function. NET25 protein level increases ~10-fold during C2C12 myoblast differentiation, and the gene is expressed at much higher levels in skeletal muscle than in most other tissues. This expression pattern is similar to that seen for the disease-linked emerin (9).

NET25 is a truncated paralog of MAN1, the factor mutated in a set of human bone density disorders (20). Both NET25 and MAN1 contain an approximately 40-residue *L*AP2-*e*merin-*M*AN1 homology domain (LEM domain) that also is found in emerin. However, outside this short region, there is no appreciable sequence conservation between emerin and NET25/MAN1. MAN1 possesses an extended C-terminal region not present in NET25 that is responsible for SMAD interaction and regulation of transforming growth factor β (TGF-β) signaling (26, 35; reviewed in reference 42). Homozygous disruption of MAN1 function in mice is embryonic lethal, and the observed vascular development defects are consistent with MAN1 function in TGF-β signaling (10, 21). Muscle function is not affected by the human disease mutations identified so far in MAN1. Nonetheless, the finding that MAN1 is expressed at much higher levels in muscle than in other tissues, similar to NET25 and emerin (9), and the observation that it binds to emerin (27) raise the possibility that MAN1 is involved in myogenesis.

In this study we use RNA interference to examine the functions of NET25 and MAN1 in the differentiation of C2C12 myoblasts, which recapitulate the basic signaling and molecular events of muscle differentiation. We find that depletion of NET25 and MAN1 strongly reduces myogenic differentiation, comparable to the inhibition of myogenesis that we observe after emerin depletion. We show that NET25 depletion causes increased extracellular signal-regulated kinase (ERK) activation within minutes of shifting cultures to differentiation conditions and that the N-terminal domain of NET25 is responsible for ERK regulation. Pharmacological rescue experiments suggest that NET25 functions in myoblast differentiation by attenuating ERK signaling. Moreover, complementation experiments with silencing-resistant human NET25 indicate that NET25 is functionally redundant with emerin in myogenic differentiation. Our work highlights both NET25 and MAN1 as novel candidate muscular dystrophy proteins. Moreover, the striking functional overlap we detect between NET25 and emerin in our myogenesis assays indicates that NET25 mutations may account for some or many of the unattributed genetic causes of EDMD.

MATERIALS AND METHODS

Cell culture, transfection, expression constructs, and RNA interference. C2C12 cells (ATCC CRL-1772) were maintained in proliferation medium (Dulbecco's modified Eagle's medium supplemented with 20% newborn calf serum, L-glutamine, sodium pyruvate, minimal essential medium nonessential amino acids, and antibiotics). For differentiation assays, cells were seeded onto gelatin-coated plates in proliferation medium (PM) at 50% confluence, grown to confluence, and then switched to differentiation medium (DM; same as PM but with 2% horse serum). This time point was considered day 0 of differentiation.

Small interfering RNAs (siRNAs) were introduced into C2C12 cells by transfecting 1.5×10^5 cells suspended in 1 ml PM, using 50 pmol siRNA and 5 μl Dharmafect 3 (Dharmacon, Lafayette, CO) per reaction. Synthetic siRNAs targeting NET25 (siNET25; M-052028-01), MAN1 (siMAN1; M-063286-00), and emerin (siEmd; M-040132-00) and a nontargeting control (D-001206-14) were from Dharmacon, each reagent consisting of a pool of four siRNAs targeting the same mRNA.

The open reading frame of human NET25 was amplified by reverse transcription-PCR from total RNA purified from the human FGM cell line with primers designed for directional insertion into pcDNA3.1D/V5-His-Topo (Invitrogen) to create pcDNA-NET25-V5. Constructs used for the deletion analysis shown in Fig. 6 were created similarly by PCR amplifying human NET25 cDNA regions encoding NET25 amino acids 1 to 404 or 199 to 503. As described above, this involved primers designed for directional insertion into pcDNA3.1D/V5-His-Topo to create pcDNA-NET25ΔC-V5 and pcDNA-NET25ΔN-V5, respectively, using pcDNA-NET25-V5 as the template. All constructs were confirmed by DNA sequencing. A stable C2C12 cell population expressing V5-tagged human NET25 was generated by bulk selection of pcDNA-NET25-V5-transfected cells with 200 μg/ml Geneticin over the course of 2 weeks.

DNA transfections were performed with 1×10^5 to 1.5×10^5 cells suspended in 1 ml PM, using 1 μg plasmid DNA and 10 μl Optifect reagent (Invitrogen, Carlsbad, CA) per reaction. After a 15-min incubation with the DNA/reagent mixture, cells were plated onto 12-well culture dishes which were precoated with gelatin for differentiation experiments or equipped with 18-mm round glass coverslips for use in immunofluorescence studies. Using a green fluorescent protein (GFP) reporter construct (pEGFP; Clontech, Mountain View, CA), we routinely achieved 70 to 90% transfection efficiency with this "reverse transfection" technique, except when cells were grown on glass coverslips for immunofluorescence studies, where transfection efficiency was typically lower (30 to 50%) (data not shown).

pENTR/U6-based plasmids for the expression of short hairpin RNAs (shRNAs) targeting NET25/1 (shNET25/1), NET25/2 (shNET25/2), MAN1 (shMAN1), emerin (shEmd), LAP2β (shLAP2β), and EGFP (shEGFP) and the empty vector control were designed and constructed according to recommendations from the vendor (Invitrogen). Recombinant purified human epidermal growth factor (rEGF) was from Cell Signal Technologies (CST; Danvers, MA). The *P* values shown in Fig. 2 and 6 were determined using an unpaired two-tailed *t* test.

Immunofluorescence microscopy and myogenic index (MI) analysis. To determine myogenic indices, knockdown and control C2C12 cultures on day 4 after shift to DM were washed thrice with phosphate-buffered saline (PBS), fixed for 10 min with 2% formaldehyde, permeabilized (10 min) with 0.1% Triton X-100, and stained with mouse anti-MyHC (M9850-15B; U.S. Biological, Swampscott, MA) primary and Alexa Fluor 488-coupled anti-mouse immunoglobulin G (Invitrogen) secondary antibodies. Nuclei were marked with Hoechst 33342 (Invitrogen). Images were acquired on a Leica DM IRE2 microscope equipped with a Hamamatsu C4742-95 digital charge-coupled-device camera. Images were analyzed using ImageJ software to determine the total number of nuclei and the number of nuclei within MyHC-positive areas.

For subcellular localization studies, cells on glass coverslips were washed, fixed with 4% formaldehyde, and permeabilized with 0.1% Triton X-100. Cells were then stained with rabbit anti-V5 tag primary antibody (Genscript, Piscataway, NJ) diluted 1:500 in PBS-3% bovine serum albumin, and then incubated with Alexa 568-coupled anti-rabbit secondary antibody. Nuclei were stained with Hoechst 33342. Samples were visualized using a 63× oil immersion objective on our Leica microscope (see above).

Western blotting and antibodies. Western blotting was performed as described in reference 37. Briefly, cells were washed with ice-cold PBS and directly dissolved into sodium dodecyl sulfate-polyacrylamide gel electrophoresis loading dye containing proteinase and phosphatase inhibitor cocktails (Roche, Indianapolis, IN). Equal cell equivalents of total protein (~20 μg) were resolved on Novex 4 to 20% Tris-glycine gels (Invitrogen) and transferred to nitrocellulose membranes. Membranes were blocked with 5% nonfat dry milk reconstituted in Tris-buffered saline buffer with 0.1% Tween 20 (TBS/T) and probed with the following primary antibodies diluted in TBS/T: mouse anti-emerin (Novocastra catalog number NCL-EMERIN), mouse antimyogenin (BD Pharmingen catalog number 556358), mouse anti-MyoD (Abcam catalog number 16148), rabbit anti-Myf-5 (Santa Cruz catalog number 302), rabbit anti-Erk1/2 (CST catalog number

9102), rabbit anti-phospho-Erk1/2 (Thr202/Tyr204; CST catalog number 9101), rabbit anti-SAPK/JNK (CST catalog number 9252), rabbit anti-phospho-SAPK/JNK (Thr183/Tyr185; CST catalog number 9251), rabbit anti-p38 (CST catalog number 9212), rabbit anti-phospho-p38 (Thr180/Tyr182; CST catalog number 9211), rabbit anti-MEK1/2 (CST catalog number 9122), rabbit anti-phospho-MEK1/2 (Ser217/221; CST catalog number 9121), mouse anti-phospho-Elk1 (Ser383; CST catalog number 9181), mouse anti-GAPDH (Abcam catalog number 9484), and rabbit anti-V5 (Genscript catalog number A00623). In-house-generated antibodies against NET25 (9), LAP2β (44), and MAN1 (this study) were affinity purified against the immunogen.

BrdU incorporation assay. C2C12 cells were transfected with siRNA as described above and seeded onto 12-well plates. Thirty-six hours later, cultures were either left in PM or shifted to DM for the times indicated (see Fig. 4), and S phase nuclei were labeled by adding 10 μM bromodeoxyuridine (BrdU) for 45 min. Cultures were fixed with 4% formaldehyde, stained with mouse monoclonal anti-BrdU antibody coupled to Alexa 594 (Invitrogen), and counterstained with Hoechst 33342. Images were acquired with our epifluorescence microscope (see above) and analyzed using ImageJ software to determine the total number of nuclei and the number of BrdU-positive nuclei.

Cell cycle analysis. siRNA-transfected and control cells were prepared for flow cytometry analysis by ethanol fixation and propidium iodide staining as described previously (41). Data were acquired on a BD FACSCalibur flow cytometer. Percentages of G_1, S, and G_2 phase cells were determined from cell cycle profiles by using the Watson pragmatic algorithm of the cell cycle platform within FlowJo software (Tree Star Inc., Ashland, OR) with the "remove doublets" and "remove debris" options enabled. *P* values were determined using an unpaired two-tailed *t* test.

Semiquantitative reverse transcription-PCR. Total mRNA from control and shRNA-transfected C2C12 cultures was prepared using the Qiagen RNeasy mini kit and reverse transcribed with the Transcriptor first-strand cDNA synthesis kit (Roche). Three microliters of cDNA was used as input for duplex PCR mixtures containing 0.2 μM of each primer for simultaneous amplification of the hypoxanthine phosphoribosyltransferase (HPRT) control and experimental mRNAs. Primers used were HPRT-F (GGATTTGAAATTCCAGACAAG TTTG), HPRT-R (AGTGCAAATCAAAAGTCTGGGG), NET25-F (TGGTT CAGGACCACTATGTGGAC), NET25-R (CGAGATTCATTGGAAGCCA), emerin-F (GTGCGTGATGACATTTTCTCT), emerin-R (GGTGGAGGATG TAGGATAATATGA), MAN1-F (GGAAATAGGAGATCACTGGCA), and MAN1-R (TTCCCAGCATATTCCGGA). Due to differences in apparent efficiency of amplification, reactions for NET25 and MAN1 were run for 30 cycles and emerin reactions for 25 cycles. Products were resolved on 6% nondenaturing polyacrylamide gels, stained with SYBR green I (Invitrogen) and visualized on a Storm 860 system by using blue fluorescence (Molecular Dynamics). Images were quantified using Imagequant software, and intensities of experimental mRNAs were normalized to those of the internal HPRT control.

Pharmacological rescue experiments. shRNA-transfected and control cells were treated singly or in combination with 10 μM U0126 (CST catalog number 9903) and SB431542 (S4317; Sigma-Aldrich, St. Louis, MO) as indicated in the text. Stock solutions of inhibitors were dissolved in 100% ethanol and diluted at least 1,000 times in serum-free medium to achieve the final concentrations. The Jun N-terminal protein kinase (JNK) inhibitor SP600125 (S5567; Sigma-Aldrich) was dissolved in dimethyl sulfoxide and diluted to achieve a final working concentration of 10 nM. Cultures were allowed to differentiate for 4 days before MI analysis (see above).

RESULTS

NET25 and MAN1 are required for efficient myoblast differentiation. To test a possible function of NET25 and MAN1 in myogenesis, we depleted these proteins from cultures of proliferating C2C12 cells by shRNA that was expressed after transfection with pENTR/U6-based expression constructs. Thirty-six hours after transfection, knockdown and control cultures were shifted to DM and assayed 4 days later for myogenic differentiation. The MI, defined as the percentage of nuclei found in MyHC-positive myotubes, was used as the measure for differentiation (Fig. 1).

Two different shRNA constructs that we utilized, shNET25/1 and shNET25/2 (from here on referred to as shNET25), each caused depletion of ~80% of the NET25 protein that appeared in control cells at day 4 (Fig. 1C). In agreement with previously published results involving NET25/Lem2 depletion in HeLa cells (41), the NE was not detectably affected by NET25 depletion in C2C12 cells, as judged by the normal localization of emerin, LAP2β, and lamins A/C to the NE (data not shown) and normal nuclear morphology (e.g., Fig. 1A). Depletion of NET25 reduced the MI to 22% and 19% for the two shRNAs, compared to 44% and 47% observed for the empty vector control and an shRNA control (shEGFP), respectively (Fig. 1A and B). Interestingly, depletion of MAN1 from C2C12 cultures (Fig. 1C) also strongly inhibited myogenesis (MI, ~14%) (Fig. 1B). Consistent with previous work showing that loss of emerin blocks myoblast differentiation in culture (18), we observed strong inhibition of myogenesis in C2C12 cultures where emerin was depleted with shRNA (MI reduced to 21%) (Fig. 1A and B).

The INM-integrated beta-isoform of LAP2 (LAP2β) (17), which also has an LEM domain, was not predicted to function in C2C12 differentiation, based on its lack of preferential expression in muscle (9). Indeed, reducing LAP2β expression with shLAP2β to the same degree as that achieved for the other three targets of interest (Fig. 1C) had no effect on myogenesis (MI = 48%). Thus, at our level of sensitivity, only three of the four LEM domain-containing proteins of the INM are important for myoblast differentiation.

Accompanying the strong reduction in myogenesis seen in cultures where NET25, emerin, and MAN1 were silenced, the level of the "late" MRF myogenin did not substantially increase in these cells during the 4-day period after shift to DM. This was in sharp contrast to the strong induction of myogenin seen in the controls and in cells treated with shLAP2β (Fig. 1D). Conversely, the levels of the early MRFs MyoD and Myf5, which promote myogenin upregulation, remained high for two or more days after shift to differentiation conditions in cultures, where NET25, emerin, and MAN1 were silenced. Therefore C2C12 cells lacking NET25, MAN1, or emerin are unable to efficiently differentiate even though early MRFs are present.

MAN1 depletion causes cell cycle alteration. Exit from the cell cycle, expression of myogenic factors, and terminal differentiation occur in a highly coordinated manner during myogenesis (2). It has been shown that expression of an LMNA mutant that causes EDMD in C2C12 cells leads to inefficient myogenic differentiation and results in improper exit from the cell cycle (16). Therefore, it was conceivable that reduction of NET25, emerin, or MAN1 levels interfered with myoblast differentiation by altering cell cycle withdrawal.

We tested this possibility by using BrdU incorporation as a measure for S phase activity. We found that depletion of NET25 and emerin had no effect on the number of BrdU-positive nuclei in proliferating or early differentiating C2C12 cultures (Fig. 2). In contrast, cultures depleted of MAN1 showed a much higher proportion of S phase nuclei than did cultures transfected with nontargeting control siRNA. This difference was clearly evident under proliferation conditions in high-serum medium and continued during the following 8 h after shift to low-serum DM. However, the rate at which the percentage of S phase nuclei decreased over the 8-h period following shift to DM was nearly identical between siMAN1 and the nontargeting control siRNA-transfected cultures.

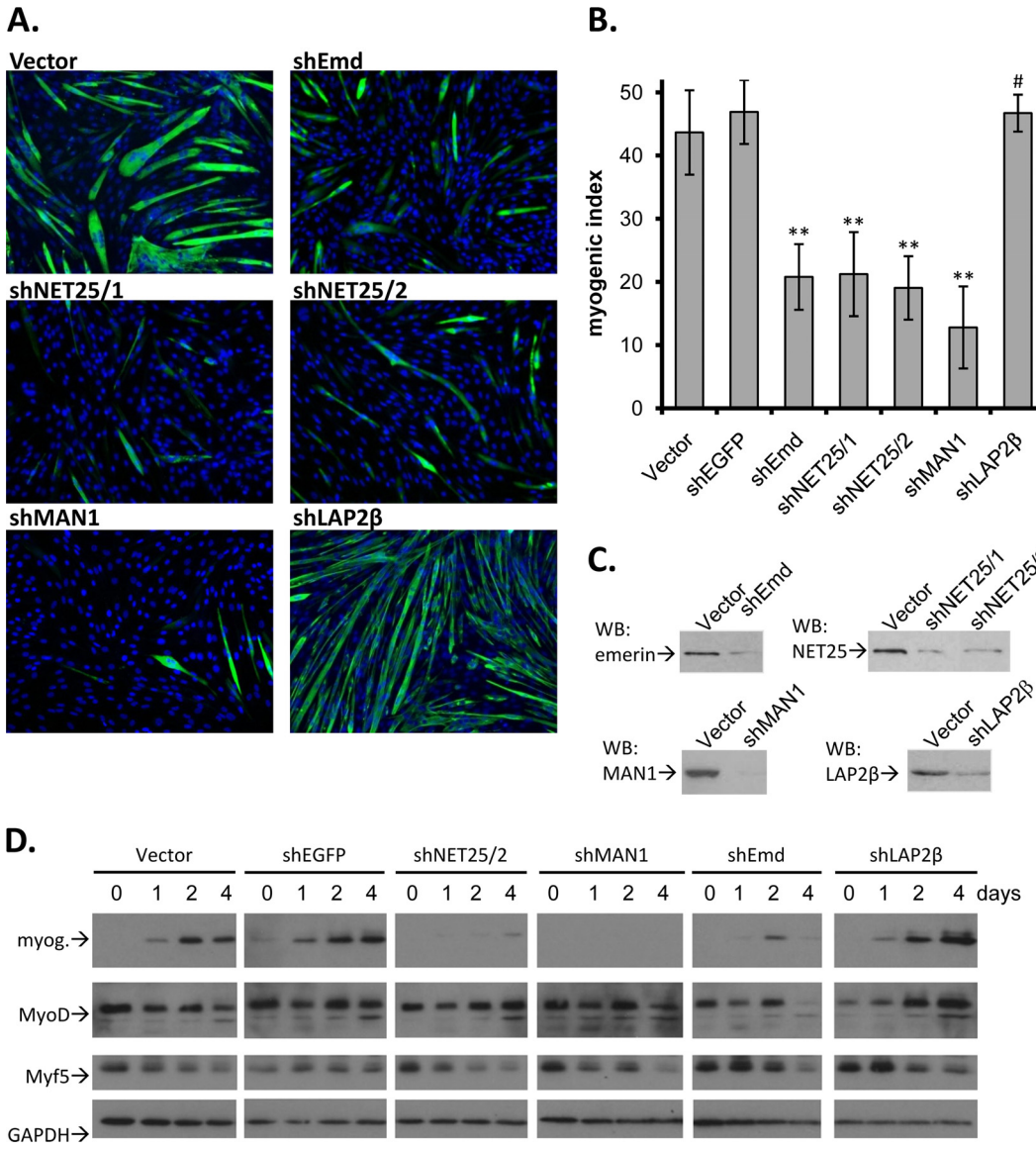

FIG. 1. Effects of depletion of NET25, emerin, MAN1, and LAP2β on C2C12 myogenic differentiation. (A) Micrographs showing immunofluorescent staining of C2C12 cells (green, MyHC; blue, DNA) transfected with empty pENTR/U6 (Vector) or pENTR/U6-derived constructs expressing shRNAs targeting emerin (shEmd), NET25 (shNET25/1, shNET25/2), MAN1 (shMAN1), or LAP2β (shLAP2β). Cultures were maintained in DM for 4 days before analysis. (B) Quantification of myogenic differentiation, involving at least four of the images shown in panel A, from at least four individual experiments. The MI is the percentage of nuclei that were found in MyHC-positive cells. Error bars indicate standard deviations. Asterisks indicate P values of $\leq 1.75 \times 10^{-4}$; the # symbol above the shLAP2β column indicates a P value of 0.378 compared to the vector control. (C) Western blot analysis (WB) of target protein depletion in shRNA-expressing C2C12 cultures. (D) Western blot analysis of myogenic markers myogenin (myog.), MyoD, and Myf5 in cultures transfected with shRNA constructs targeting NET25, MAN1, emerin, or LAP2β. A time course over 4 days is shown. GAPDH levels are shown as a loading control.

Moreover, the total number of cells did not increase in siMAN1 compared to control cultures, measured by quantifying the number of nuclei per field of view (data not shown). Therefore, despite the increase in the percentage of S phase cells in cultures depleted of MAN1, there was no apparent effect on the kinetics of cell cycle exit.

We confirmed and extended these results by analyzing the cell cycle profiles of propidium iodide-stained C2C12 cells by using flow cytometry (Fig. 2D and E). Again, the cell cycle distributions of siNET25- and siEmd-transfected cells were not markedly different from the control cultures. However, siMAN1-transfected cultures showed a statistically significant increase in S phase cells by 16% relative to the control, and a decrease of the G_1 population by 16.9%. G_2 populations were not significantly affected by any of the targeting shRNAs compared to the control. This suggests that the increase in S phase cells in shMAN1 cultures may be due to premature exit from the G_1 phase.

NET25 complements the myogenic function of emerin but not that of MAN1. Since NET25, emerin, and MAN1 are all

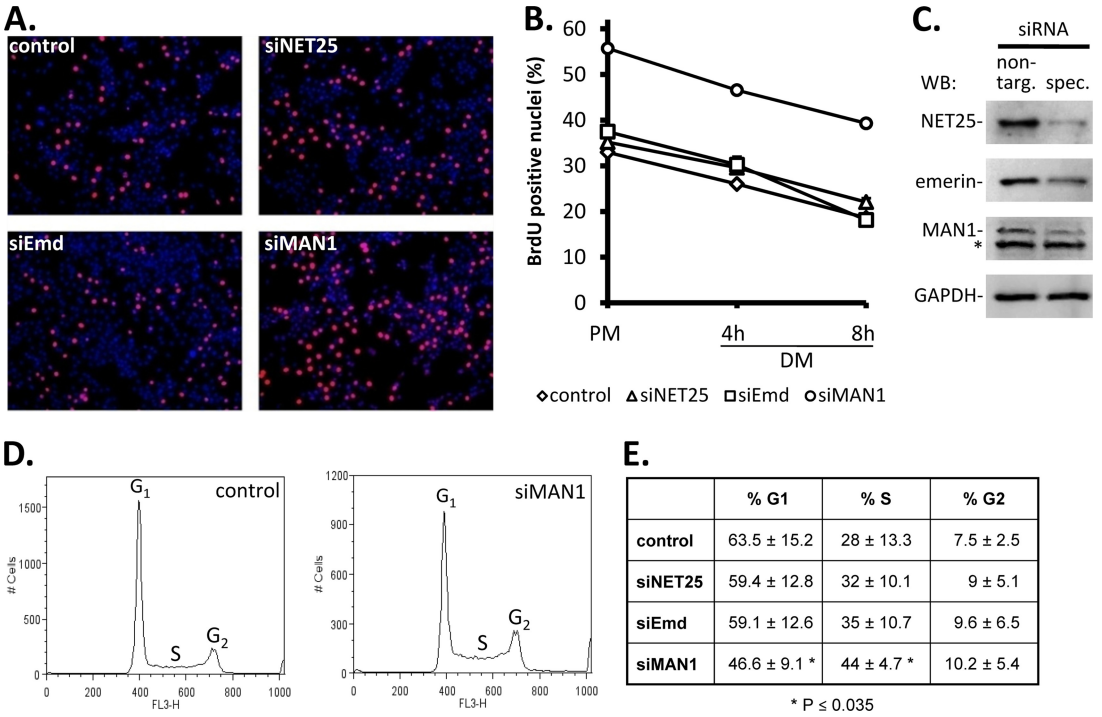

	% G1	% S	% G2
control	63.5 ± 15.2	28 ± 13.3	7.5 ± 2.5
siNET25	59.4 ± 12.8	32 ± 10.1	9 ± 5.1
siEmd	59.1 ± 12.6	35 ± 10.7	9.6 ± 6.5
siMAN1	46.6 ± 9.1 *	44 ± 4.7 *	10.2 ± 5.4

* P ≤ 0.035

FIG. 2. Effects of depletion of NET25, emerin, and MAN1 on cell cycle in C2C12 cultures. (A) Immunofluorescent micrographs from a BrdU incorporation assay of C2C12 cultures (red, BrdU; blue, DNA) transfected with a nontargeting control siRNA or with siRNAs targeting NET25 (siNET25), emerin (siEmd), or MAN1 (siMAN1). Images shown correspond to the 4-h DM time point in panel B. (B) Quantification of BrdU-positive nuclei in control and NET25-, emerin-, or MAN1-depleted C2C12 cultures over a time course of 8 h after shift from PM to DM. (C) Western blot analysis (WB) confirming knockdown of the target proteins by siRNA. Protein extracts were prepared at the time of shifting cultures to DM. Left lane, protein levels after transfection with nontargeting control siRNA (non-targ.); right lane, protein levels after transfection with specific siRNA (spec.) targeting NET25, emerin, or MAN1. Blots were probed with antibodies recognizing the siRNA targets as indicated on the left. A nonspecific band on the MAN1 Western blot is marked by an asterisk. A GAPDH loading control representative of even loading in all panels is shown at the bottom. (D) Cell cycle profiles of control and siMAN1-transfected C2C12 cells in PM, 36 h after transfection. Representative examples are shown. Labels mark the cell populations in the G_1 (left peak), S (saddle), and G_2 (right peak) phases of the cell cycle based on their DNA content. (E) Summary of cell cycle distributions in control and siRNA-transfected C2C12 cells. Percentages shown are averages of the results for at least four experiments ± the standard deviations. Asterisks mark values with statistically highly significant differences in comparison to the control ($P \leq 0.035$).

required for myogenesis (Fig. 1), we analyzed whether they are functionally redundant in this process. For this, we created a C2C12 cell population that stably expressed human NET25 tagged with the V5 epitope (Fig. 3B). Despite good conservation between mouse and human NET25 proteins at the amino acid level (83% identity), human NET25 mRNA was not predicted to be targeted by shNET25 due to its nucleotide sequence variation.

Expression of V5-tagged human NET25 was clearly evident in the stably transfected cell population and was not detected in the empty vector control (Fig. 3B). Human NET25-V5 protein expression was not affected by shNET25 (Fig. 3B), which reduced endogenous murine NET25 mRNA levels by at least 77% (Fig. 3C, top). shEmd and shMAN1 had no significant effect on the levels of either V5-tagged human NET25 protein or endogenous NET25 mRNA (Fig. 3B and C), but reduced levels of emerin and MAN1 mRNA, respectively, by at least 64% (Fig. 3C, middle and bottom). MI analysis revealed that human NET25 restored myogenic differentiation to approximately wild-type levels in shNET25- and shEmd-transfected cultures, but it failed to rescue myogenesis in shMAN1-transfected cultures (Fig. 3A). This strongly suggested that the functions of NET25 and emerin are redundant in myogenesis, despite that fact that they have no apparent homology outside the short LEM domain. Conversely, MAN1 has relatively strong homology to NET25 throughout most of its sequence, but must have at least partially unique functions in myogenic differentiation that cannot be complemented by its paralog, at least with the levels of ectopic expression achieved here.

NET25 depletion elevates ERK signaling. Upregulation of ERK signaling in cardiomyocytes from emerin null mice as well as in emerin-depleted C2C12 cells has been reported recently (30, 31). Given the importance of mitogen-activated protein kinase (MAPK) signaling in cell differentiation, and based on our complementation studies with human NET25, we hypothesized that NET25 also might play a role in regulating ERK signaling during myogenesis. We analyzed phospho-MAPK activation in C2C12 cultures that were depleted of NET25 by semiquantitative Western blotting with antibodies specific for only the activated phosphorylated forms, and antibodies that recognize both activated and nonactivated forms of the kinases (Fig. 4). These experiments revealed that after shift to DM, control C2C12 cells experience rapid albeit transient activation of ERK1/2 and stress-activated protein kinase

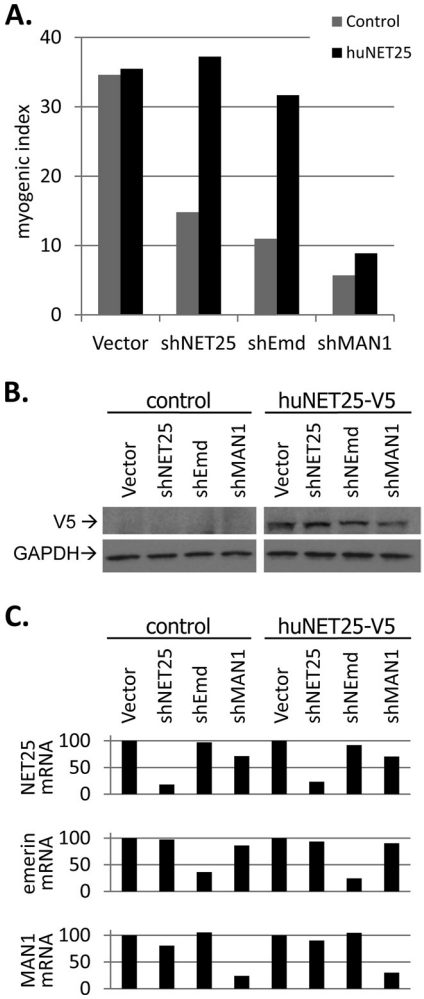

FIG. 3. Rescue of differentiation by complementation with human NET25. (A) MI analysis of nontransfected control C2C12 cultures (gray bars) and C2C12 cultures expressing human NET25-V5 (black bars) after transfection with the empty vector control (Vector) or plasmids expressing shRNAs against NET25 (shNET25/1, shNET25/2), emerin (shEmd), or MAN1 (shMAN1). Cultures were allowed to differentiate for 4 days before MI analysis. Representative data from one out of three individual experiments are shown. (B) Western blot analysis of V5-tagged human NET25 protein levels in control C2C12 cultures (control; corresponding to gray bars in panel A) and C2C12 cultures stably transfected with pcDNA-NET25-V5 (huNET25-V5; corresponding to black bars in panel A). Transfection with vector control and shRNA constructs targeting endogenous NET25, emerin, and MAN1 is indicated above each gel lane. GAPDH levels are shown as a loading control. (C) mRNA levels of endogenous NET25 (top), emerin (middle), and MAN1 (bottom) in control and human NET25-V5-expressing C2C12 cultures after transfection with shRNA constructs. Values shown were normalized against the internal HPRT control, and "vector" control levels were set to 100%.

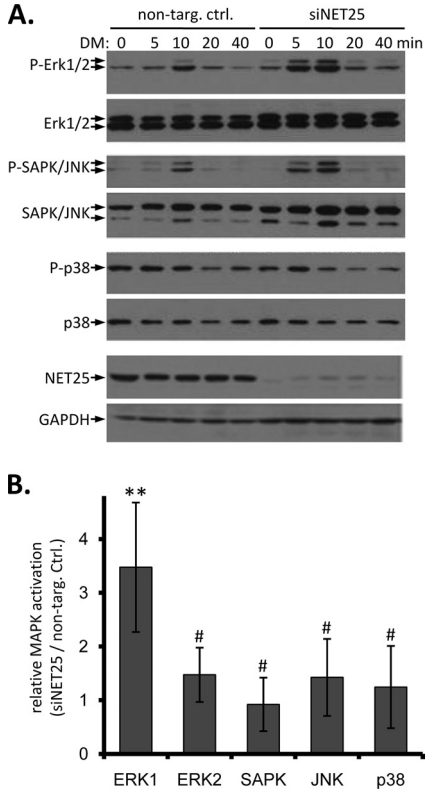

FIG. 4. MAPK activation in C2C12 cells at the onset of differentiation after NET25 depletion. (A) Western blot analysis of the three major branches of MAPK signaling in C2C12 cells transfected with a nontargeting control siRNA (non-targ. ctrl.) or with siRNA targeting NET25 (siNET25), between 0 and 40 min after shift to differentiation conditions. Antigens detected in each panel are indicated to the left. Activated phosphorylated forms of MAPKs are indicated by the prefix "P-." NET25 depletion was confirmed by Western blotting (second panel from bottom). GAPDH is shown as a loading control. (B) Relative activation of MAPKs in NET25-depleted cultures compared to control C2C12 cultures. Phospho-MAPK levels were normalized against total MAPK levels at the 10-min time point after shift to DM and values from NET25-depleted samples divided by values from nontargeting control samples. Numbers shown were calculated from the averages of the results for at least four independent experiments, one of which is shown in panel A. Error bars indicate standard deviations. Asterisks indicate a statistically significant difference between siNET25 and control data sets in ERK1 activation ($P = 0.027$). The # symbol above all other columns indicates P values of ≥ 0.452.

and/or JNK, with a peak of activation 10 min after shift. Similar short-term ERK activation has been described in epithelial cells in response to EGF (32) and also in response to Wnt as a result of signaling pathway cross talk (1).

Significantly, siNET25 cultures showed a much stronger induction of ERK1 and also slightly stronger induction of ERK2 phosphorylation following shift to DM (Fig. 4A, right side) than did the control cultures. At the peak of MAPK activation (10 min after shift to DM), relative phospho-ERK1 levels were 3.5-fold higher in NET25-depleted cultures than in cultures transfected with the nontargeting control siRNA (Fig. 4B). The effect of NET25 depletion on phospho-ERK2 levels and on the phosphorylation of the other MAPKs tested ranged from 0.9- to 1.5-fold, indicating that NET25 preferentially affects ERK1 activation. We were able to recapitulate recently published results from Muchir et al. (30) as an experimental control and found hyperactivation of ERK1 (twofold) and ERK2 (1.2-fold) at 10 min after shift of emerin-depleted cultures to differentiation conditions (data not shown). This draws another striking parallel between emerin and NET25 functions at the molecular level.

In order to confirm that NET25 functions in the canonical ERK pathway, we tested the response of control and NET25-

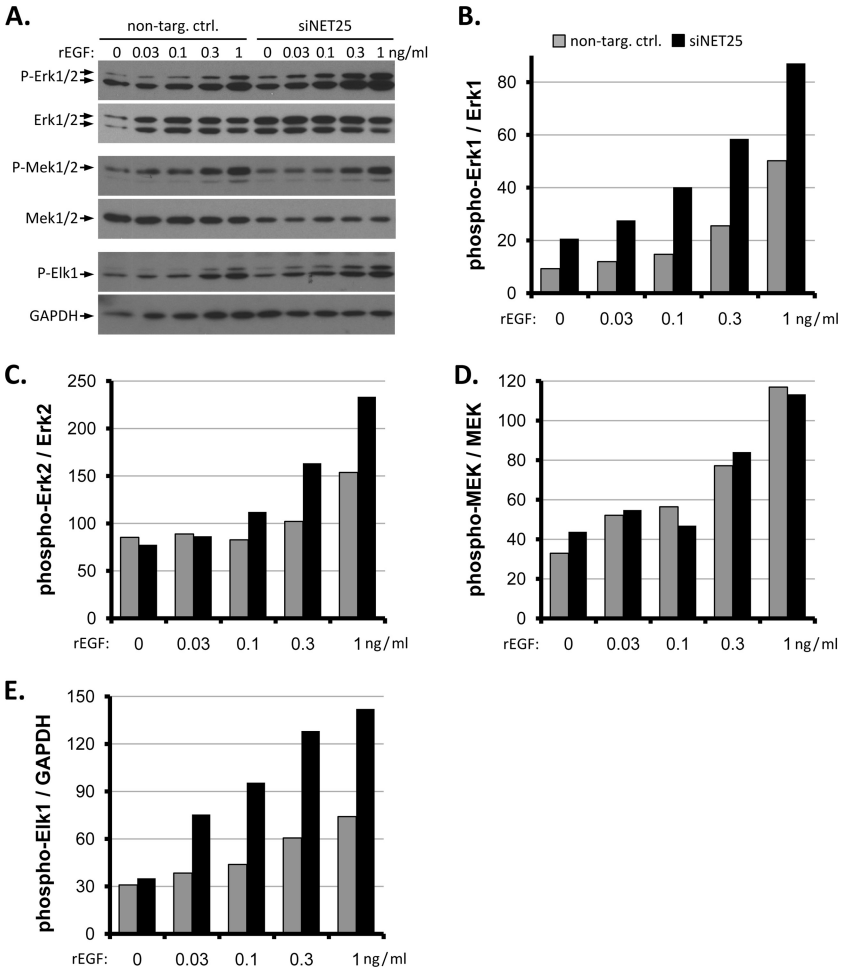

FIG. 5. Response of NET25-depleted C2C12 cultures to EGF. (A) Western blot analysis of activation of the ERK1/2 cascade in response to rEGF in nontargeting control and siNET25-transfected C2C12 cultures. Final concentrations of rEGF are indicated above each gel lane. Antibodies used are indicated to the left. (B to E) Quantification of phosphorylated ERK1, phosphorylated ERK2, phosphorylated MEK1/2, and phosphorylated Elk1 levels normalized against total kinase levels and GAPDH signals. Representative data from one out of three individual experiments are shown.

depleted C2C12 cultures to rEGF (Fig. 5). We found that phospho-ERK1 levels were 1.7- to 2.7-fold higher in siNET25 cultures than in control cultures at all of the applied EGF concentrations relative to the nontreated control (Fig. 5B). In this experiment, phospho-ERK2 levels were again slightly elevated at the higher EGF concentrations tested, but the effect was not as dramatic as that observed for ERK1 (Fig. 5C).

Upregulation of phospho-ERK1 levels in response to NET25 depletion could indicate that NET25 positively affects upstream components of the signaling cascade. However, in NET25-depleted cultures, the levels of phospho-MEK1/2 (the kinase immediately upstream of ERK in the kinase cascade) were unchanged (Fig. 5D). In contrast, the phosphorylated form of Elk1, a direct substrate of ERK1/2, was enhanced upon stimulation with rEGF in siNET25 cultures (Fig. 5E). These results suggest that NET25 depletion leads to ERK pathway activation that extends into compartments downstream of ERK1/2, but does not affect the cascade upstream of ERK1/2.

The N terminus of NET25 is required for ERK regulation. In order to map the region of NET25 that is required for regulation of ERK activation, we created two deletion constructs based on the human NET25 sequence (Fig. 6A). pcDNA-NET25ΔC-V5 (see Materials and Methods) programmed the expression of a V5 epitope-tagged NET25 version that lacks the nucleoplasmic region downstream of the second predicted transmembrane segment of NET25. pcDNA-NET25ΔN-V5 specified expression of V5-tagged NET25 lacking the N-terminal nucleoplasmic region upstream of the first predicted transmembrane segment of NET25, including the LEM domain (Fig. 6A and B). The truncations were designed to retain 10 amino acids after the second transmembrane region (pcDNA-NET25ΔC-V5) and 10 amino acids before the first transmembrane region (pcDNA-NET25ΔN-V5) to promote proper transmembrane topology of these constructs. Subcellular localization of full-length and truncated NET25 proteins in C2C12 cells was determined by fluorescence microscopy with anti-V5 antibody (Fig. 6C). NET25 and NET25ΔC were clearly localized to the nuclear rim and also were present in cytoplasmic aggregates. A similar level of nuclear rim staining was observed for NET25ΔN, although in this

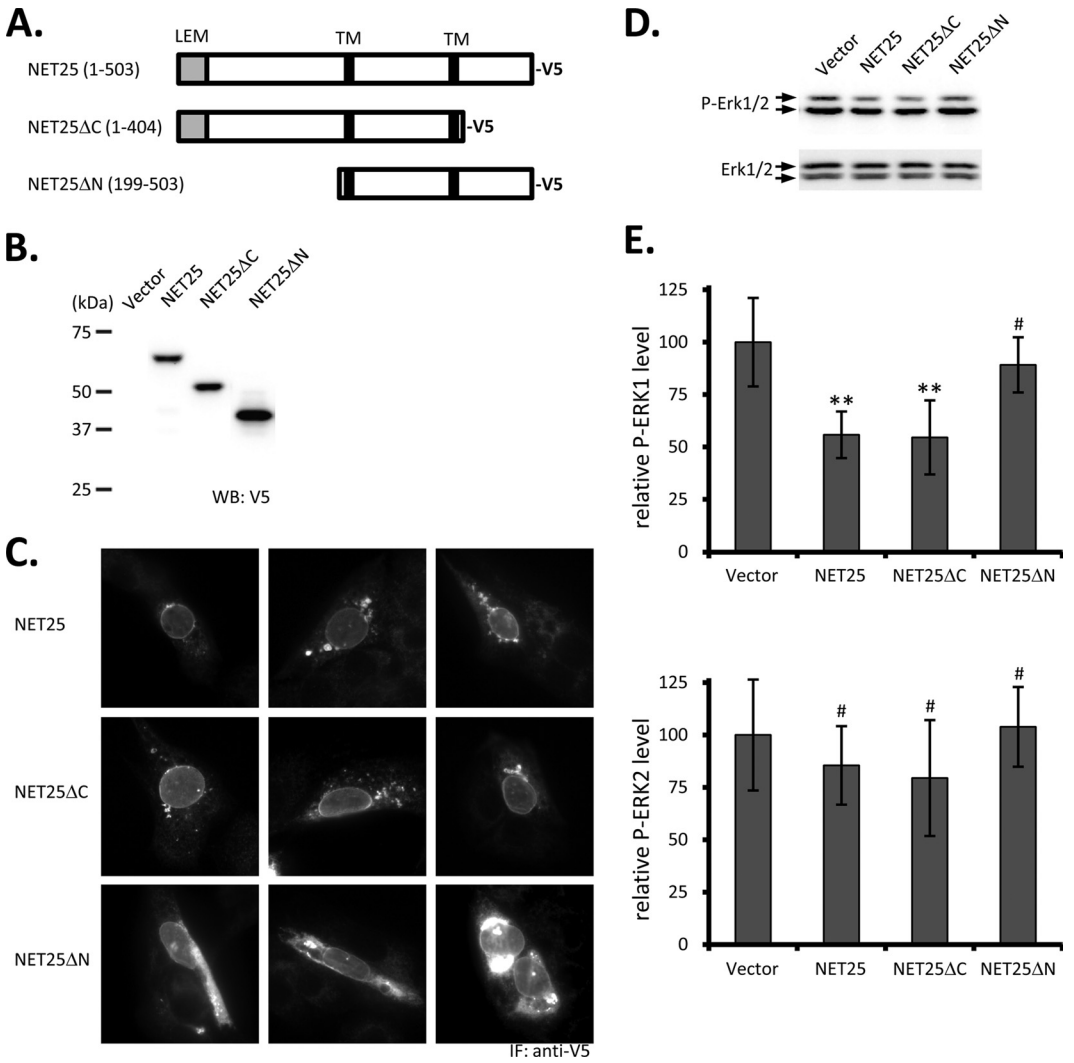

FIG. 6. ERK activation in C2C12 cells after overexpression of NET25, NET25ΔC, and NET25ΔN. (A) Schematic of the full-length and truncated NET25 proteins used in these experiments. Numbers in parentheses indicate amino acid regions of human NET25 expressed in the resulting recombinant protein. The C-terminal V5 tag is indicated. (B) Western blot analysis of expression of full-length and truncated NET25 in C2C12 cells. Samples were probed with anti-V5 antibody to detect the tagged fusion proteins. (C) Immunofluorescence (IF) microscopy analysis of V5-tagged NET25, NET25ΔC, and NET25ΔN localization. Three representative images are shown for each construct. (D) Example of a semiquantitative Western blot analyzing ERK activation after treating NET25-, NET25ΔC-, or NET25ΔN-expressing C2C12 cells with 0.3 mg/ml rEGF for 15 min. (E) Graphs summarizing quantification of ERK1 (top) and ERK2 activation (bottom) from at least four experiments. Error bars indicate standard deviations. Asterisks mark statistically significant differences in comparison to the vector control ($P \leq 0.006$). The # symbol indicates P values of ≥ 0.354.

case, more and larger cytoplasmic aggregates were detected. This difference may have been a consequence of the expression level of NET25ΔN being higher than that NET25 and NET25ΔC, which we observed by Western blotting (Fig. 6B).

We assayed relative phospho-ERK1 and phospho-ERK2 levels after stimulation with 0.3 ng/ml EGF in cells expressing full-length or truncated NET25, 36 h after transfection with the respective expression constructs or the empty vector control. As shown in Fig. 6D and E, expression of full-length NET25 and NET25ΔC significantly reduced ERK1 activation to 56% ($P = 0.04$) and 55% ($P = 0.06$), respectively, relative to the vector control. In contrast, ERK1 activation was not significantly affected by the expression of NET25ΔN (89%; $P = 0.41$). These data indicate that the N-terminal nucleoplasmic domain of NET25 is required to modulate ERK1 activation. In agreement with our previous result involving NET25 silencing (Fig. 4), we were not able to detect a significant effect for either NET25, NET25ΔC, or NET25ΔN on ERK2 activation in this overexpression approach (Fig. 6D, bottom; all P values, ≥ 0.43).

Inhibition of ERK signaling restores myogenesis after NET25 and emerin depletion. Because hyperactivation of ERK signaling within the first few minutes after shift to differentiation conditions appeared to interfere with myogenesis, we tested to see if transient suppression of this MAPK signaling pathway could correct the myogenic defect after NET25 and emerin depletion. We used the highly specific and potent MEK1/2 inhibitor U0126 (14) to transiently abolish ERK1/2

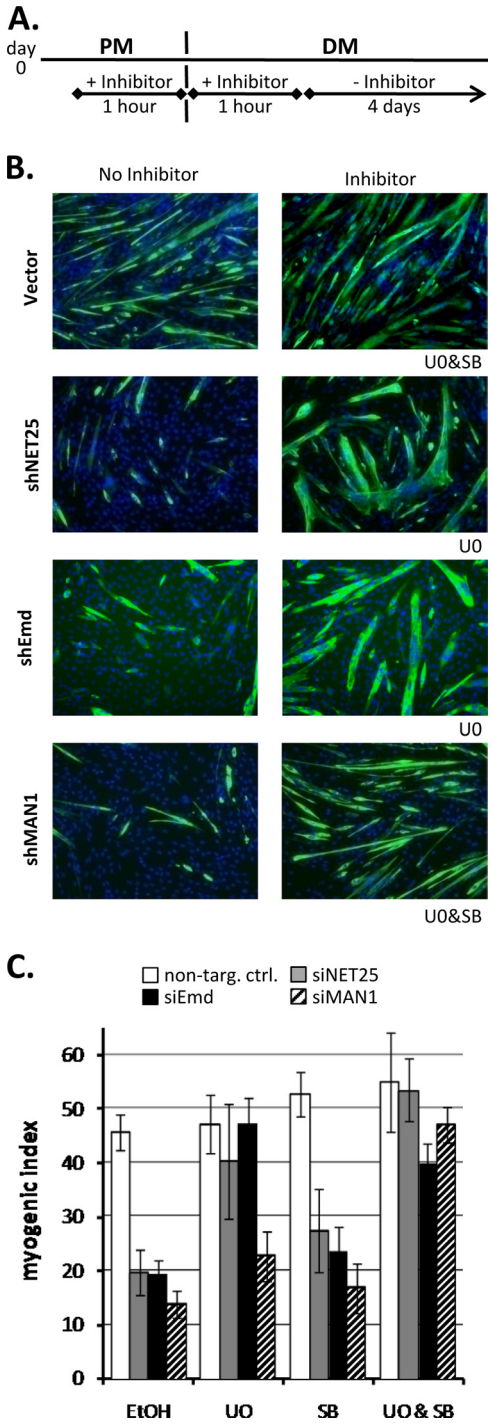

FIG. 7. Pharmacological rescue of myogenic defect in C2C12 cultures after depletion of NET25, emerin, and MAN1. (A) Schematic of the time course of inhibitor application. On day 0, proliferating C2C12 cultures were treated with an inhibitor for the period between 1 h before and 1 h after shifting cells from PM to DM. Cultures were then kept for 4 days in DM before MI analysis. (B) Immunofluorescent micrographs (green, MyHC; blue, DNA) of empty vector control (Vector) and NET25 (shNET25)-, emerin (shEmd)-, or MAN1 (shMAN1)-depleted C2C12 cultures treated with MEK1/2 inhibitor U0126 (U0) and/or TGF-β inhibitor SB431542 (SB). The inhibitor applied to the drug-treated cultures (right column) is indicated below the bottom right corner of each image. Cultures were assayed after 4 days of differentiation. Images shown are from one representative experiment. (C) MI analysis of NET25 (gray bars)-, emerin (black bars)-, and MAN1 (hatched bars)-depleted as well as control (open bars) cultures treated with U0 and/or SB. Average values from the results for at least three independent experiments are shown. Error bars indicate standard deviations.

phosphorylation at the time of shift to DM (Fig. 7). In a related approach, pharmacological inhibition with the MEK1/2 inhibitor PD98059 has been shown to improve differentiation of myoblasts from *Lmna*(*R453W*) mutant mice (15). Initial optimization showed that treatment of the cultures with 10 μM U0126 from 1 h before shift until 1 h after shift to DM (Fig. 7A) showed the greatest effect on the MI in NET25-depleted cultures. In contrast, a continuous presence of U0126 over the entire course of a differentiation experiment (4 days) was toxic to C2C12 cells (data not shown). The efficacy of U0126 in C2C12 cells was confirmed by semiquantitative Western blot analysis of phospho-ERK1/2 levels (data not shown).

Myogenic differentiation in shNET25 and shEmd cultures (MIs of 20% and 19%, respectively, compared to 45% in the control) was almost completely restored by U0126 to levels comparable to that of the drug-treated, nondepleted control (MIs of 40% and 47%, respectively, compared to 47% in the control; Fig. 7B and C). On the other hand, U0126 had only a small positive effect on the MI in MAN1-depleted C2C12 cultures. Because MAN1 regulates SMAD signaling (21, 26), we also tested the effect of SB431542, a specific inhibitor of the TGF-β receptor serine/threonine kinase activity, on myogenesis in NET25-, emerin-, and MAN1-depleted cultures. SB431542 alone had little or no effect on the MI in shNET25, shEmd, and shMAN1 cultures. However, a combination of the MEK1/2 and TGF-β receptor inhibitors completely restored differentiation of MAN1-depleted cultures. Hence, transient ablation of ERK1/2 phosphorylation alone is enough to rescue the NET25 and emerin defect, but transient inhibition of both ERK signaling and TGF-β/SMAD signaling is required to overcome the MAN1 defect. This provided an additional line of evidence that NET25 and emerin functions in myogenesis at least partially overlap and that they are separable from MAN1 functions.

Whereas NET25 depletion substantially increased the activation of ERK kinases after shift of myoblasts to DM, a more modest activation of JNK also was observed (Fig. 4). To investigate whether this was functionally significant, we tested whether the JNK inhibitor SP600125 could restore myogenesis. However, using the same regimen of drug exposure as that used for the ERK inhibitor, we found no effect of SP600125 on myogenesis in shNET25-transfected cultures (data not shown).

DISCUSSION

Transmembrane proteins of the INM are a functionally diverse group of components that interact closely with lamins. Previously, emerin was the only transmembrane protein of the INM implicated in myogenesis (18). Here, using C2C12 cells, we show that NET25 and MAN1 are two additional INM proteins required for myogenic differentiation. These three proteins all regulate cell signaling (26, 30, 31, 35; also, this

study), and the results of our phenotypic analysis highlight the importance of their signaling functions in myogenic differentiation. Our results, in concert with other recent data, support the model that diseases caused by NE mutations can at least partially result from changes in signaling pathways.

Surprisingly, we found that emerin and NET25 have redundant functions in myoblast differentiation. The sequence homology between NET25 and emerin is limited to the LEM domain in the first ~40 amino acids, and the transmembrane topology of NET25 (a type III/multipass transmembrane protein) is different from that of emerin (a type II/single-pass transmembrane protein). Nonetheless, the silencing of NET25 and emerin showed identical phenotypic signatures in cell differentiation, cell cycle, and MAPK activation assays. More importantly, increasing NET25 levels by ectopic overexpression compensated for loss of emerin function in myogenesis. Furthermore, pharmacologically suppressing the burst of ERK1/2 activity that occurred shortly after shift to DM was sufficient to restore myogenesis in both NET25- and emerin-depleted cultures. Therefore, NET25 and emerin appear to have overlapping functions in myogenesis by regulation of ERK signaling (see below).

Despite the relatively strong amino acid sequence similarity of 57% between MAN1 and NET25 (6), the effects of MAN1 depletion on C2C12 cells were distinct from those seen with NET25 and emerin depletion in three ways. First, only silencing of MAN1 caused an increase in the percentage of S phase nuclei in proliferating and early differentiating cell cultures, even though cell cycle exit was not impaired. This increase came at the expense of the G_1 population in MAN1-depleted cultures, suggesting that lower MAN1 levels cause cells to enter S phase prematurely. Second, ectopic expression of NET25 did not rescue myogenesis after MAN1 depletion. Third, although pharmacological suppression of ERK signaling alone was sufficient to rescue myogenesis in NET25- and emerin-silenced cultures, the combined inhibition of ERK and SMAD signaling was needed to restore myogenic differentiation in shMAN1 cultures. Therefore, NET25 and MAN1 have at least partially nonredundant functions in differentiation of C2C12 cells. The pharmacological rescue experiments further suggest that MAN1 not only regulates TGF-β signaling (reviewed in reference 3), but also can influence ERK signaling, either directly or via cross talk with the TGF-β pathway.

Our conclusion that NET25 regulates ERK is supported by four lines of evidence. First, the levels of phospho-ERK1, and to a lesser degree the levels of phospho-ERK2, are elevated in NET25-depleted cultures relative to those in control C2C12 cultures shortly after shifting cultures to DM. Second, ERK1, and to a lesser extent ERK2, was more sensitive to activation by EGF in NET25-depleted C2C12 cultures. Third, overexpression of human NET25 in C2C12 cells diminished ERK1 activation in response to EGF. Fourth, a pharmacological approach showed that the myogenic defect in NET25-depleted myoblast cultures can be rescued by transient inhibition of ERK phosphorylation at the onset of myogenesis.

Both the amplitude as well as the duration of MAPK signaling can influence the physiological outcome of pathway activation (28). In addition, regulation of spatial distribution of signaling components can alter the output of a signaling event, such as by regulating access to substrates (13). NET25 and emerin could play roles in either scenario. Transient hyperactivation of ERK1/2 occurring in the absence of NET25 or emerin could directly upregulate expression of antimyogenic factors or inactivate promyogenic factors, thus derailing the myogenic program. Proliferation of muscle progenitor cells (satellite cells) in response to mitogens, predominantly hepatocyte growth factor and fibroblast growth factor (FGF) family members, involves ERK activation via receptor tyrosine kinases and is required for efficient muscle repair in vivo (8). However, uncontrolled proliferation of muscle progenitor cells is incompatible with myogenesis, consistent with studies showing that constitutive activation of MAPK signaling by forced expression of Ras inhibits myogenic differentiation of C2C12 cells (11). Therefore, proliferative signals have to be turned off after myoblast expansion in order to allow formation of muscle fibers. The switch from proliferation to differentiation could be promoted by mammalian Sprouty isoforms, which negatively regulate FGF-2 mediated ERK activation (34). Overexpression of Sprouty-2 allows C2C12 differentiation in the presence of FGF-2 (12), and Sprouty homologs 1, 2, and 3 are transcriptionally upregulated during C2C12 differentiation (9; also see GEO accession number GSE4694). Analogously, NET25 and emerin could aid myogenesis by keeping ERK1/2 signals in check at the initial stages of terminal differentiation emulated by the C2C12 model system used here. This proposition agrees with our previous observation that NET25 levels are highest in adult mouse muscle (9), where it might help to maintain a nonproliferative state.

Mechanistically, our data indicate that NET25 acts at or very close to the level of ERK1 in this signaling cascade. In NET25-depleted cells in which ERK1 was hyperactivated, we found that MEK1/2, the MAPK that activates ERK1/2, itself was not hyperactivated, unlike a downstream target of ERK1 (Elk1). Our deletion analysis revealed that the N-terminal nucleoplasmic domain of NET25 is required for the suppression of ERK1 activation by NET25, whereas the C-terminal nucleoplasmic domain, predicted to form a winged helix domain akin to the one found in MAN1 (7), is not required. It is noteworthy that the N-terminal region of NET25 contains several features that indicate a potentially direct interaction with ERK1. The Scansite web server (33) identifies residues 89 to 103 and 216 to 230 of mouse NET25 as potential ERK docking (ERK-D) sites, a motif that confers physical interaction with ERKs (39). Moreover, residue Ser97 in mouse NET25 is predicted to be phosphorylated by ERK1. Although we have not yet been able to obtain conclusive evidence that NET25 physically interacts with ERK1 or one of its phosphatases, we propose that NET25 could function as a scaffold that brings ERK1 and a cognate MAPK phosphatase into close proximity at the nuclear periphery and thus attenuates ERK signaling. Analysis of the NE proteome and NET25 protein interactions in myonuclei will address this possibility in the future.

In conclusion, our study suggests that the LEMD2 gene (encoding NET25) is an excellent candidate for a novel disease gene within the large cohort of EDMD cases that cannot be attributed to mutations in EMD or LMNA. Analysis of NET25 in EDMD patients and animal models of muscular dystrophy could provide insight into this question in the near future.

ACKNOWLEDGMENTS

We thank the members of our laboratory for critical discussion of the manuscript.

This work was supported by NIH grant RO1 GM28521 to L.G. M.D.H. was supported by NIH fellowship F32 GM080045.

REFERENCES

1. **Almeida, M., L. Han, T. Bellido, S. C. Manolagas, and S. Kousteni.** 2005. Wnt proteins prevent apoptosis of both uncommitted osteoblast progenitors and differentiated osteoblasts by beta-catenin-dependent and -independent signaling cascades involving Src/ERK and phosphatidylinositol 3-kinase/AKT. J. Biol. Chem. **280:**41342–41351.
2. **Andrés, V., and K. Walsh.** 1996. Myogenin expression, cell cycle withdrawal, and phenotypic differentiation are temporally separable events that precede cell fusion upon myogenesis. J. Cell Biol. **132:**657–666.
3. **Bengtsson, L.** 2007. What MAN1 does to the Smads. TGFbeta/BMP signaling and the nuclear envelope. FEBS J. **274:**1374–1382.
4. **Bione, S., E. Maestrini, S. Rivella, M. Mancini, S. Regis, G. Romeo, and D. Toniolo.** 1994. Identification of a novel X-linked gene responsible for Emery-Dreifuss muscular dystrophy. Nat. Genet. **8:**323–327.
5. **Bonne, G., M. R. Di Barletta, S. Varnous, H. M. Becane, E. H. Hammouda, L. Merlini, F. Muntoni, C. R. Greenberg, F. Gary, J. A. Urtizberea, D. Duboc, M. Fardeau, D. Toniolo, and K. Schwartz.** 1999. Mutations in the gene encoding lamin A/C cause autosomal dominant Emery-Dreifuss muscular dystrophy. Nat. Genet. **21:**285–288.
6. **Brachner, A., S. Reipert, R. Foisner, and J. Gotzmann.** 2005. LEM2 is a novel MAN1-related inner nuclear membrane protein associated with A-type lamins. J. Cell Sci. **118:**5797–5810.
7. **Caputo, S., J. Couprie, I. Duband-Goulet, E. Konde, F. Lin, S. Braud, M. Gondry, B. Gilquin, H. J. Worman, and S. Zinn-Justin.** 2006. The carboxyl-terminal nucleoplasmic region of MAN1 exhibits a DNA binding winged helix domain. J. Biol. Chem. **281:**18208–18215.
8. **Chargé, S. B., and M. A. Rudnicki.** 2004. Cellular and molecular regulation of muscle regeneration. Physiol. Rev. **84:**209–238.
9. **Chen, I. H., M. Huber, T. Guan, A. Bubeck, and L. Gerace.** 2006. Nuclear envelope transmembrane proteins (NETs) that are up-regulated during myogenesis. BMC Cell Biol. **7:**38.
10. **Cohen, T. V., O. Kosti, and C. L. Stewart.** 2007. The nuclear envelope protein MAN1 regulates TGFbeta signaling and vasculogenesis in the embryonic yolk sac. Development **134:**1385–1395.
11. **Conejo, R., C. de Alvaro, M. Benito, A. Cuadrado, and M. Lorenzo.** 2002. Insulin restores differentiation of Ras-transformed C2C12 myoblasts by inducing NF-kappaB through an AKT/P70S6K/p38-MAPK pathway. Oncogene **21:**3739–3753.
12. **de Alvaro, C., N. Martinez, J. M. Rojas, and M. Lorenzo.** 2005. Sprouty-2 overexpression in C2C12 cells confers myogenic differentiation properties in the presence of FGF2. Mol. Biol. Cell **16:**4454–4461.
13. **Ebisuya, M., K. Kondoh, and E. Nishida.** 2005. The duration, magnitude and compartmentalization of ERK MAP kinase activity: mechanisms for providing signaling specificity. J. Cell Sci. **118:**2997–3002.
14. **Favata, M. F., K. Y. Horiuchi, E. J. Manos, A. J. Daulerio, D. A. Stradley, W. S. Feeser, D. E. Van Dyk, W. J. Pitts, R. A. Earl, F. Hobbs, R. A. Copeland, R. L. Magolda, P. A. Scherle, and J. M. Trzaskos.** 1998. Identification of a novel inhibitor of mitogen-activated protein kinase kinase. J. Biol. Chem. **273:**18623–18632.
15. **Favreau, C., E. Delbarre, J. C. Courvalin, and B. Buendia.** 2008. Differentiation of C2C12 myoblasts expressing lamin A mutated at a site responsible for Emery-Dreifuss muscular dystrophy is improved by inhibition of the MEK-ERK pathway and stimulation of the PI3-kinase pathway. Exp. Cell Res. **314:**1392–1405.
16. **Favreau, C., D. Higuet, J. C. Courvalin, and B. Buendia.** 2004. Expression of a mutant lamin A that causes Emery-Dreifuss muscular dystrophy inhibits in vitro differentiation of C2C12 myoblasts. Mol. Cell. Biol. **24:**1481–1492.
17. **Foisner, R., and L. Gerace.** 1993. Integral membrane proteins of the nuclear envelope interact with lamins and chromosomes, and binding is modulated by mitotic phosphorylation. Cell **73:**1267–1279.
18. **Frock, R. L., B. A. Kudlow, A. M. Evans, S. A. Jameson, S. D. Hauschka, and B. K. Kennedy.** 2006. Lamin A/C and emerin are critical for skeletal muscle satellite cell differentiation. Genes Dev. **20:**486–500.
19. **Gueneau, L., R. B. Yaou, L. Demay, S. Llense, N. Deburgrave, F. Leturcq, P. Richard, and G. Bonne.** 2006. G.P. 4.09 Looking for a third gene causing Emery-Dreifuss muscular dystrophy: lessons and perspectives. Neuromuscul. Disord. **16:**677–678.
20. **Hellemans, J., O. Preobrazhenska, A. Willaert, P. Debeer, P. C. Verdonk, T. Costa, K. Janssens, B. Menten, N. Van Roy, S. J. Vermeulen, R. Savarirayan, W. Van Hul, F. Vanhoenacker, D. Huylebroeck, A. De Paepe, J. M. Naeyaert, J. Vandesompele, F. Speleman, K. Verschueren, P. J. Coucke, and G. R. Mortier.** 2004. Loss-of-function mutations in LEMD3 result in osteopoikilosis, Buschke-Ollendorff syndrome and melorheostosis. Nat. Genet. **36:**1213–1218.
21. **Ishimura, A., J. K. Ng, M. Taira, S. G. Young, and S. Osada.** 2006. Man1, an inner nuclear membrane protein, regulates vascular remodeling by modulating transforming growth factor beta signaling. Development **133:**3919–3928.
22. **Kuang, S., K. Kuroda, F. Le Grand, and M. A. Rudnicki.** 2007. Asymmetric self-renewal and commitment of satellite stem cells in muscle. Cell **129:**999–1010.
23. **Lammerding, J., J. Hsiao, P. C. Schulze, S. Kozlov, C. L. Stewart, and R. T. Lee.** 2005. Abnormal nuclear shape and impaired mechanotransduction in emerin-deficient cells. J. Cell Biol. **170:**781–791.
24. **Lammerding, J., R. D. Kamm, and R. T. Lee.** 2004. Mechanotransduction in cardiac myocytes. Ann. N. Y. Acad. Sci. **1015:**53–70.
25. **Lammerding, J., P. C. Schulze, T. Takahashi, S. Kozlov, T. Sullivan, R. D. Kamm, C. L. Stewart, and R. T. Lee.** 2004. Lamin A/C deficiency causes defective nuclear mechanics and mechanotransduction. J. Clin. Investig. **113:**370–378.
26. **Lin, F., J. M. Morrison, W. Wu, and H. J. Worman.** 2005. MAN1, an integral protein of the inner nuclear membrane, binds Smad2 and Smad3 and antagonizes transforming growth factor-beta signaling. Hum. Mol. Genet. **14:**437–445.
27. **Mansharamani, M., and K. L. Wilson.** 2005. Direct binding of nuclear membrane protein MAN1 to emerin in vitro and two modes of binding to barrier-to-autointegration factor. J. Biol. Chem. **280:**13863–13870.
28. **Marshall, C. J.** 1995. Specificity of receptor tyrosine kinase signaling: transient versus sustained extracellular signal-regulated kinase activation. Cell **80:**179–185.
29. **Muchir, A., G. Bonne, A. J. van der Kooi, M. van Meegen, F. Baas, P. A. Bolhuis, M. de Visser, and K. Schwartz.** 2000. Identification of mutations in the gene encoding lamins A/C in autosomal dominant limb girdle muscular dystrophy with atrioventricular conduction disturbances (LGMD1B). Hum. Mol. Genet. **9:**1453–1459.
30. **Muchir, A., P. Pavlidis, G. Bonne, Y. K. Hayashi, and H. J. Worman.** 2007. Activation of MAPK in hearts of EMD null mice: similarities between mouse models of X-linked and autosomal dominant Emery Dreifuss muscular dystrophy. Hum. Mol. Genet. **16:**1884–1895.
31. **Muchir, A., W. Wu, and H. J. Worman.** 2009. Reduced expression of A-type lamins and emerin activates extracellular signal-regulated kinase in cultured cells. Biochim. Biophys. Acta **1792:**75–81.
32. **Murphy, L. O., S. Smith, R. H. Chen, D. C. Fingar, and J. Blenis.** 2002. Molecular interpretation of ERK signal duration by immediate early gene products. Nat. Cell Biol. **4:**556–564.
33. **Obenauer, J. C., L. C. Cantley, and M. B. Yaffe.** 2003. Scansite 2.0: proteome-wide prediction of cell signaling interactions using short sequence motifs. Nucleic Acids Res. **31:**3635–3641.
34. **Ozaki, K.-i., S. Miyazaki, S. Tanimura, and M. Kohno.** 2005. Efficient suppression of FGF-2-induced ERK activation by the cooperative interaction among mammalian Sprouty isoforms. J. Cell Sci. **118:**5861–5871.
35. **Pan, D., L. D. Estevez-Salmeron, S. L. Stroschein, X. Zhu, J. He, S. Zhou, and K. Luo.** 2005. The integral inner nuclear membrane protein MAN1 physically interacts with the R-Smad proteins to repress signaling by the transforming growth factor-β superfamily of cytokines. J. Biol. Chem. **280:**15992–16001.
36. **Pasotti, M., C. Klersy, A. Pilotto, N. Marziliano, C. Rapezzi, A. Serio, S. Mannarino, F. Gambarin, V. Favalli, M. Grasso, M. Agozzino, C. Campana, A. Gavazzi, O. Febo, M. Marini, M. Landolina, A. Mortara, G. Piccolo, M. Vigano, L. Tavazzi, and E. Arbustini.** 2008. Long-term outcome and risk stratification in dilated cardiolaminopathies. J. Am. Coll. Cardiol. **52:**1250–1260.
37. **Sambrook, J., E. F. Fritsch, and T. Maniatis.** 1989. Molecular cloning: a laboratory manual, 2nd ed., vol. 3. Cold Spring Harbor Laboratory Press, Cold Spring Harbor, NY.
38. **Schirmer, E. C., L. Florens, T. Guan, J. R. Yates III, and L. Gerace.** 2003. Nuclear membrane proteins with potential disease links found by subtractive proteomics. Science **301:**1380–1382.
39. **Sharrocks, A. D., S. H. Yang, and A. Galanis.** 2000. Docking domains and substrate-specificity determination for MAP kinases. Trends Biochem. Sci. **25:**448–453.
40. **Stewart, C. L., K. J. Roux, and B. Burke.** 2007. Blurring the boundary: the nuclear envelope extends its reach. Science **318:**1408–1412.
41. **Ulbert, S., W. Antonin, M. Platani, and I. W. Mattaj.** 2006. The inner nuclear membrane protein Lem2 is critical for normal nuclear envelope morphology. FEBS Lett. **580:**6435–6441.
42. **Worman, H. J.** 2006. Inner nuclear membrane and regulation of Smad-mediated signaling. Biochim. Biophys. Acta **1761:**626–631.
43. **Worman, H. J., and G. Bonne.** 2007. "Laminopathies": a wide spectrum of human diseases. Exp. Cell Res. **313:**2121–2133.
44. **Yang, L., T. Guan, and L. Gerace.** 1997. Integral membrane proteins of the nuclear envelope are dispersed throughout the endoplasmic reticulum during mitosis. J. Cell Biol. **137:**1199–1210.